J. Fluid Mech. (1987), *vol.* 178, *pp.* 379–403
Printed in Great Britain

Diffusion of matter by a non-buoyant plume in grid-generated turbulence

By IKUO NAKAMURA,
Department of Mechanical Engineering, Nagoya University, Nagoya 464, Japan

YASUHIKO SAKAI
The College of General Education, Nagoya University, Nagoya 464, Japan

AND MASAFUMI MIYATA
Department of Mechanical Engineering, Yamanashi University, Kofu 400, Japan

(Received 28 May 1985 and in revised form 6 October 1986)

The turbulent diffusion process is investigated for a continuous point source of a non-buoyant plume in grid-generated water turbulence. Two kinds of biplanar grids with a mesh length of 10 mm and 20 mm were used. The mesh Reynolds numbers were 1480 and 2970, respectively. The mean and fluctuating concentration fields of aqueous dye solution were measured by the light absorption method. Experimental results for both grids were compared.

For both grids, the mean concentration radial profiles proved to have a similar Gaussian shape, and the mean concentration on the plume axis obeys the hyperbolic decay law well. These mean concentration profiles and their decay show an excellent agreement with the results deduced from the similarity analysis for the mean concentration field.

Radial profiles of the fluctuation r.m.s. value and relative intensity (i.e. the ratio of the r.m.s. value to the mean concentration) were found also to be nearly similar, and the centreline r.m.s. value decays downstream as a hyperbola. The relative intensity on the centreline tends to increase slightly downstream. All experimental results obtained were much less scattered and more reliable than those reported earlier.

The similarity for the concentration fluctuation intensity has been analysed using a thin-layer approximation. Also, an approximate analysis of the fluctuating concentration field is given by replacing the fluctuating concentration signal by a randomly spaced sequence of rectangular waves with various heights and widths.

1. Introduction

The study of the diffusion of passive scalars in turbulent flows forms a foundation for understanding various turbulence phenomena, and has practical importance for dispersions of pollutants, mixing of materials and chemical reactions.

Experimental studies on the diffusion of a scalar quantity in turbulent flow can be classified broadly into two categories: the study of diffusion in shear flows, or in a flow field without mean shear. The present experiment belongs to the latter category. With respect to the type of source or diffusion field, the study of a diffusion field without mean velocity shear could be divided into the study of a statistically homogeneous scalar field and that concerning diffusion from an instantaneous or

continuous line or point source. Since Taylor (1921), the homogeneous scalar field has been studied mainly for its theoretical interest in connection with turbulent statistical theory (e.g. Hinze 1975, pp. 278–305; Batchelor & Townsend 1956; Batchelor 1952). However, the present study will be somewhat different from those studies in which the focus is on the statistics of the homogeneous scalar fluctuation field where the mean spread of a scalar field is immaterial. Since this is surely important for engineering applications the homogeneous scalar problem will not be mentioned here.

Experimental or theoretical studies on the diffusion of heat from a continuous line source have long been undertaken for grid-generated turbulence, as in Uberoi & Corrsin (1953) and Townsend (1954). Uberoi & Corrsin (1953) investigated the spread of the mean temperature and profiles of the fluctuation intensity downstream of the heated wire, estimating the Lagrangian velocity correlation for heated fluid particles, Lagrangian integral and micro scales. Townsend (1954) examined the similarity in the diffusion process of heat and the effect of the molecular diffusivity on the spread of heated fluid particles in the downstream area not far from the line source. The diffusion of heat from a heated line source stretched in a core region of pipe flow was investigated by Baldwin & Mickelsen (1962) and Crum & Hanratty (1965). Further, in connection with meteorology, the diffusion of a fluorescent tracer material released from an aircraft along a predetermined line at right angles to the wind was investigated by Csanady, Hilst & Bowne (1968).

More recent developments will be given below where appropriate.

Many studies on the diffusion from a continuous point source have been made in various velocity fields (i.e. uniform mean velocity flow, grid turbulence, pipe flow, lake and ocean, etc.). Regarding the uniform mean velocity field or grid turbulence, the experiment by Kampe de Feriet (1938) seems to be the first, in which small soap bubbles were released from a fixed point source. Kalinske & Pien (1944) performed diffusion experiments in a water channel by injecting a mixture of carbon tetrachloride and benzene with the same density as water, which formed small droplets in the water. To investigate the contribution of molecular diffusion to the total mean dispersion at long diffusion times, Mickelsen (1960) compared the lateral dispersion of helium and carbon dioxide downstream from a continuous point source in the turbulence produced by a grid in a wind tunnel.

Recent studies on grid turbulence were reported by Yamamoto & Sato (1979), Gad-el-Hak & Morton (1979) and Britter *et al.* (1983). Yamamoto & Sato (1979) introduced polystyrene particles into grid-generated water turbulence and investigated the trajectory of a tracer particle by pursuing its motion with an optical method. Gad-el-Hak & Morton (1979) studied the downstream evolution of smoke released in grid air turbulence by a laser-scattering method. Britter *et al.* (1983) studied the diffusion of dye solution from a continuous point source in a stably stratified saline–water solution.

In the core region of turbulent pipe flow, the mean concentration fields for diffusion from the continuous point source were investigated by Towle & Sherwood (1939), Towle, Sherwood & Seder (1939), and MacCarter, Stutzman & Koch (1949). Relatively recently, measurements, including the concentration fluctuations, have been made by Lee & Brodkey (1964), Nye & Brodkey (1967*a*) and Becker, Rosensweig & Gwozdz (1966). In the experiments of Lee & Brodkey (1964) and Nye & Brodkey (1967*a*), dye solution was used as the diffusing matter, and the concentration fluctuations and spectra were measured by the light absorption method. Becker *et al.* (1966) examined a plume of oil smoke particles (Coray 55) in pipe air flow by the

light-scattering method, clarifying the effect of Reynolds number (481000–684000) on the fluctuation-intensity profile and spectra distributions.

The diffusion from a point source in lakes and the atmosphere has come into the limelight in connection with environmental pollution. Actual flows in the environment have almost mean shear, and flow without the shear, as in the present experiments, is rather rare. However, as examples akin to diffusion in the no-shear flow field, the studies by Csanady (1966), Murthy & Csanady (1971) and Ramsdell & Hinds (1971) can be cited; Csanady (1966) and Murthy & Csanady (1971) have measured the distributions of mean concentration and mean-square fluctuation for a diffusion plume of fluorescent dye (Rhodamine B) in Lake Huron, while Ramsdell & Hinds examined the diffusion process of ^{85}Kr in the atmosphere.

The purpose of this study is to present precise data on the mean concentration and concentration fluctuation in the asymptotic stage of the development (i.e. the so-called self-preserving region) of the plume from a point source in grid-generated turbulence. The reliability of the data obtained was ascertained by comparison with similar solutions on the basis of the gradient type of transport theory and models for the decay of variance. The reason why the measuring region was limited to the region far downstream of the source is that, near the source, the diffusion field is affected by the source size (Durbin 1980; Fackrell & Robins 1982), the initial injection velocity and injection method of diffusion matter, and so cannot be regarded as being from a 'point' source, which is the subject of this study. Thus, our attention will be directed only to the region where the spread of the plume is much larger than the source size, and the evolution process of the plume is not subject to the direct influence of the source conditions. It should be noted here that, when the diffusion matter was injected into the test section, the flow field was inevitably more or less disturbed whatever the injection method might be. In this experiment, particular attention will be given to the injection method so as to reduce the disturbance effect at the source as much as possible.

Remarkable developments in understanding the diffusion process of heat from a line source have been accomplished recently from both theory and experiments. In the following will be presented a summary of this development. In the previously mentioned studies, experimental investigations had mainly concerned the mean value and variance of the scalar quantity, but the exact theoretical understanding of how these properties evolve had not been achieved. However, very recently, such theoretical tools as two-particle dispersion theory (Durbin 1980; Lundgren 1981; Lamb 1981; Sawford 1983) and an approach using the joint probability density function between velocity and temperature (Anand & Pope 1984) have been developed and have thrown a new light on this problem. Detailed experimental information on how a thermal field behaves very close to a source has been given recently by Stapountzis *et al.* (1986). Further, Warhaft (1984) has examined in detail the evolution of the mean and variance of the thermal field from the near region to the region very far downstream of a line source, although the distance from the grid to the line source varied. In the light of these recent developments regarding the plume from a line source, the behaviour of the concentration field close to the line source has been considerably clarified both theoretically and experimentally. Hence, at the present time, for line sources uncertainties remain in the behaviour of the plume in the far-downstream region rather than in the near-region (see data of Warhaft 1984). On the other hand, the data on point sources are very scanty, so no comparison has been made between the above-mentioned theories and experimental results.

The noteworthy previous study on diffusion from a continuous point source in grid turbulence by Gad-el-Hak & Morton (1979) is the only one of its kind. However, owing to the disturbance effect of the source mentioned earlier and the difficulty in obtaining the concentration fluctuation measurements, the data obtained were very scattered even in the self-preserving region, so it is difficult to draw quantitative conclusions from their results. Although for diffusion with a concentration field similar to the plume in grid turbulence, the diffusion of matter from a continuous point source in the core region of the turbulent pipe flow has been examined (Lee & Brodkey 1964; Nye & Brodkey 1967*a*, Becker *et al.* 1966), there still exists a non-uniformity of several percentage points for the mean velocity even in the core region, and no satisfactory similarity of the concentration-fluctuation-intensity profile was obtained.

Studies of the concentration fluctuation field have been hindered by a paucity of suitable instrumentation for a long time. Recently, a light-scattering method (Gad-el-Hak & Morton 1979; Becker *et al.* 1966), a laser-Raman scattering method (Birch *et al.* 1978) and a heat tagging method (Belorgey, Nguyen & Trinite 1979) have been developed. In the present work, a modified light probe (Nakamura, Miyata & Sakai 1983) was used that detects a wider range of concentration than the earlier light probe (Lee & Brodkey 1963; Nye & Brodkey 1967*b*).

The importance of the present work is that, in comparison with the other studies, more precise and reliable data for the mean and fluctuating concentration fields could be obtained on the plume from a point source in grid turbulence. Attention should be, of course, focused on the behaviour of the concentration fluctuations rather than on the mean concentration properties. The fluctuation results should be of wider interest, in association with the structure of the plume in other shear flows (for example, Fackrell & Robins 1982 for the boundary layer, Nakamura *et al.* 1986 and Sakai *et al.* 1986 for the uniform mean shear flow) and practical problems such as the diffusion of the smoke from a chimney into the atmospheric boundary layer and the diffusion of pollutants from a river into the sea.

2. Experimental apparatus and conditions

A plume of dye solution from a continuous point source in grid-generated water turbulence was established in the test section of an open channel designed to measure the concentration of matter with the light absorption method. An optical method was used to detect the concentration of matter. In order to shut off the light noise from the outside, the whole channel was covered by a blackout curtain. The test section was 250 mm high, 250 mm wide and 1960 mm long. The water depth at the test section could be adjusted by controlling the heights of two weirs downstream and upstream of the grid. The end of the contraction part was equipped with suction boxes to prevent separation of the boundary layer developed on the sidewall. A three-dimensional traversing mechanism for a laser–Doppler velocimeter, light probe and hot-film probe covered 600 mm downstream, 180 mm horizontally and 250 mm vertically.

Figure 1 shows a sketch of the grids used and the coordinate systems. In this study, two biplanar grids are employed: the rod diameter d and mesh length M are $d = 2.0$ mm and 4.0 mm, $M = 10$ mm and 20 mm, respectively. For accurate assembly of grids, straight stainless-steel rods were thrust into grooves which were cut precisely by a milling machine. Mesh Reynolds numbers, $Re_M = U_0 M/\nu$, were about 1480 and 2970 for grids with $M = 10$ mm and 20 mm, respectively (hereafter,

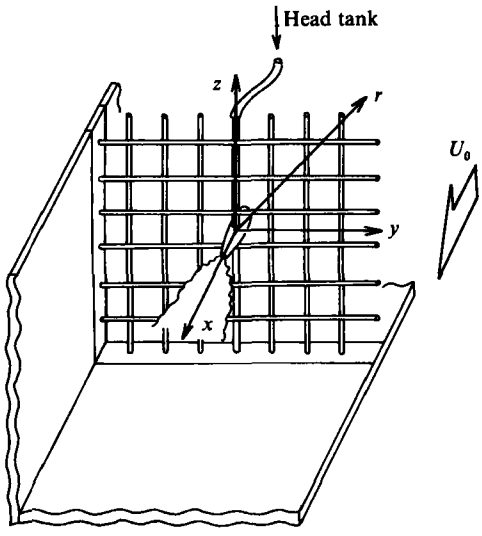

FIGURE 1. Dimensions of biplanar grids and coordinate system: d, rod diameter; M, mesh length; Re_M, Reynolds number $= U_0 M/\nu$.

$M = 10$ mm and $M = 20$ mm will be abbreviated to $M10$ and $M20$), where Re_M was evaluated with a mean velocity U_0 of 14.7 cm/s and kinematic viscosity ν of 1.004×10^{-6} m^2/s for water. These mesh Reynolds numbers seem rather low. The decay of turbulent fluctuations in this grid turbulence will be investigated later and, using an empirical decay law, the downstream variation of the longitudinal dissipation length and Reynolds number of turbulence will also be predicted. The water level in the working section was precisely adjusted to 169 ± 0.2 mm from the bottom by detecting the height of the water surface with sensing elements.

In the earlier experiments (Mickelsen 1960; Yamamoto & Sato 1979; Gad-el-Hak & Morton 1979), diffusion materials were released from an injection pipe inserted directly from the outside into the flow field, either upstream or just downstream of a grid. To obtain a better axisymmetric concentration field in the present study, two methods for releasing diffusing matter were employed: from a nozzle or an injection pipe. The nozzle was soldered to a pipe, which replaced one of the vertical rods for each grid (see Figure 1). The two nozzles used have the same exit diameter, 2 mm, and their exits are located 20 mm and 30 mm downstream of grids $M10$ and $M20$, respectively. The outer diameters of the nozzles are 4 and 6 mm for $M10$ and $M20$, and their outer shapes are streamlined. The injection pipe has an 'L' shape, and was made by bending a stainless-steel pipe with outer and inner diameters of 5 and 4 mm, respectively. At the end of the pipe, other pipes with smaller outer diameters were conjointed. The distance between the corner and exit is 120 mm. As with previous studies, the injection pipe was inserted vertically into the flow field and its exit location positioned 16 mm upstream of the grid. The dye solution is poured into the pipe through a rubber tube from the head tank.

As shown in figure 1, the coordinate system x, y, z, r is used. For an injection pipe, the coordinate origin was an intersecting point of the grid plane and the plume axis.

Figure 2 shows the injection system for the diffusion material. An aqueous solution of D.F. Orange (direct dye) was used (Nakamura *et al.* 1983) as the diffusing matter. The exact value of diffusivity for this dye solution is unknown, but it is expected to be of order 10^{-10} m^2/s (Lee & Brodkey 1964).

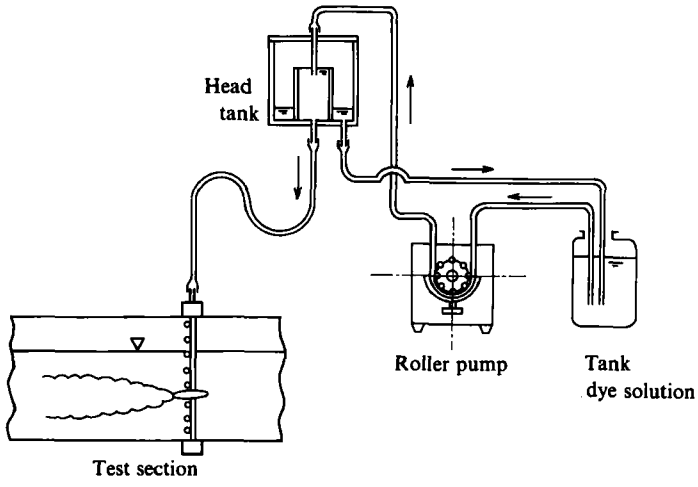

FIGURE 2. Injection system for diffusion material.

Figure 3 shows a schematic of the light probe. The diameter bundle of the optical glass is 0.5 mm and the sampling length is adjusted to about 0.7 mm. Therefore, the sampling volume is 1.37×10^{-4} c.c. (see Nakamura *et al.* 1983). The output signals of the concentration-measuring circuit were recorded over 150 s using a data recorder (SONEY, Type FR-3215W; the high cut-off frequency is 10 kHz). The time averages of the output were taken, in parallel with measurements with a mean-voltage meter mainly composed of a VF-converter (BURR-BROWN, VFC32KP) and a frequency-counting circuit. The average time is 120 s, and the mean concentrations were obtained by subtracting the mean value of zero-levels at the start and the end of each measurement from the output of the mean-voltage meter. R.m.s. values were measured with a HAYAKAWA Model HC-29 r.m.s. voltmeter with a response of at least 100 kHz (3 dB down frequency), the output of which were averaged with the mean-voltage meter over 120 s.

In the experiments, a uniform mean velocity field is indispensable to obtain a good axisymmetric concentration field. The mean velocity fields were measured for both $M10$ and $M20$ by a laser-Doppler velocimeter at a location of $x = 400$ mm. The outputs of the tracker-type signal processor (KANOMAX, Model 27-1090A) were averaged with the mean-voltage meter over 80 s. A wide region of uniform mean velocity was found in a central part of the channel.

The downstream variation in the velocity fluctuation intensity $\overline{u_x^2}$ was measured by a cylinder type of hot-film probe (TSI, Model 1212-60W; nominal frequency response 10 kHz; the diameter and length of the sensing part are $\phi 152$ μm and 2 mm, respectively) in conjunction with a constant-temperature velocity anemometer (HAYAKAWA, Model HC-30). The output of the anemometer was directly processed by a computer (NEC, PC9801) with a 2 ms sampling time, and the total number of discrete data points for one record was 20480.

Figure 4 shows the decay of the turbulent fluctuations for both the $M10$ and $M20$ grids. Also shown are other researcher's results for comparison. The present data can be adequately represented for both grids by the following power law:

$$\frac{\overline{u_x^2}}{U_0^2} = 5.66 \times 10^{-2} \left(\frac{x}{M-3} \right)^{-1.45}. \tag{1}$$

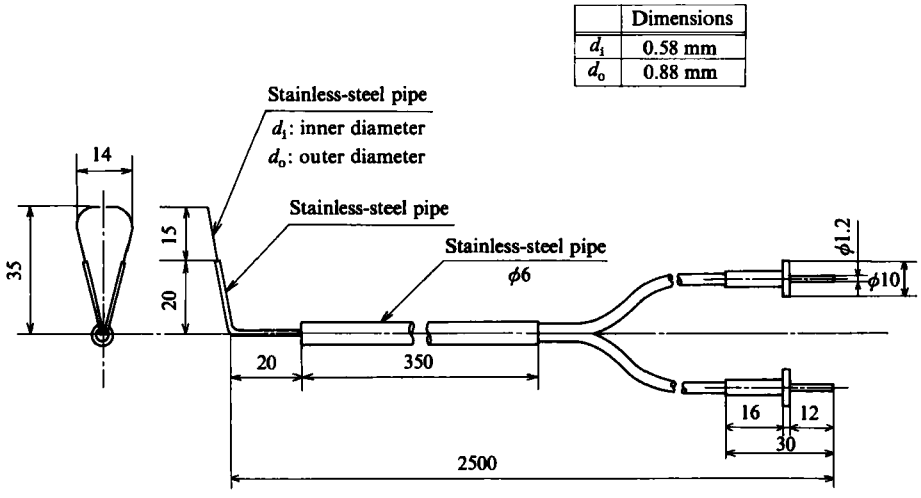

FIGURE 3. Schematic sketch of the light probe.

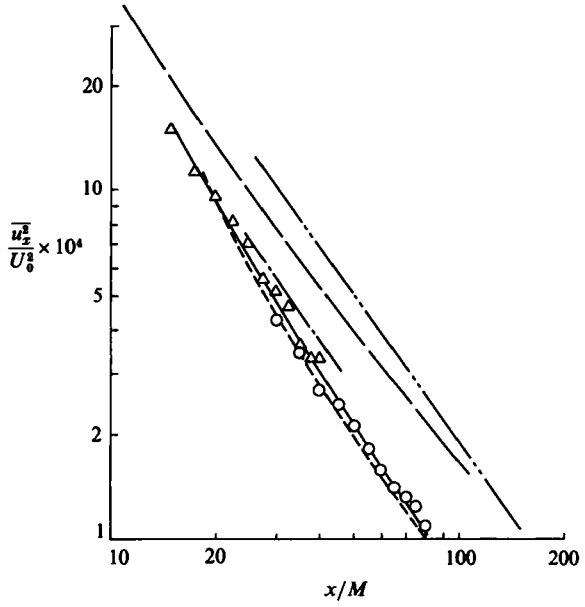

FIGURE 4. Downstream variation of $\overline{u_x^2}/U_0^2$. ○, $M = 10$ mm; △, $M = 20$ mm; ——, $0.0566(x/M-3)^{-1.45}$; -----, Batchelor & Townsend (1948) $0.0208(x/M-8)^{-1.25}$, which is given by Comte-Bellot & Corrsin (1966); —·—, Yeh & Van Atta (1973); ––, Sreenivasan *et al.* (1980) $0.04(x/M-3)^{-1.20}$; – – –, Warhaft (1984) $0.121(x/M)^{-1.4}$.

Assuming the decay of isotropic turbulence, the energy dissipation rate can be estimated as $\epsilon = -\frac{3}{2}U_0(\mathrm{d}\overline{u_x^2}/\mathrm{d}x)$, so from (1) we have

$$\epsilon = 1.23 \times 10^{-1} \frac{U_0^3}{M}\left(\frac{x}{M-3}\right)^{-2.45}. \tag{2}$$

The lateral dissipation scale λ_g, calculated from (1) and (2) and $\epsilon \approx 15\nu\overline{u_x^2}/\lambda_g^2$, is

$$\lambda_g^2 \approx 6.90 M^2 Re_M^{-1} \frac{x}{M-3}. \tag{3}$$

The Reynolds number of turbulence Re_λ varies downstream as follows:

$$Re_\lambda = (\overline{u_x^2})^{\frac{1}{2}} \lambda_g / \nu = 0.625 Re_M^{\frac{1}{2}} \left(\frac{x}{M-3} \right)^{-0.225}, \tag{4}$$

which is obtained from (1) and (3).

It should be noted here that the measured concentration fields are greatly influenced by the wake of the injection pipe or nozzles. First we investigated the horizontal profiles of the mean velocity downstream of the conduit part of the injection pipe and nozzle exits for both grids at a location of $x = 30M$, when the dye solution was injected into the flow field. Consequently, the mean velocity deficits caused by the wakes of each nozzle could be controlled easily to within 2.0% of the main mean velocity by adjusting the injection velocity of dye solution, but in the case of an injection pipe an unavoidable maximum velocity deficit of about 5% was observed in the wake of the conduit pipe, because the pipe was inserted directly into the flow field.

Next, to select a more appropriate method of introducing dye solution, the horizontal and vertical mean concentration profiles at various locations of $26.5 \leqslant x/M \leqslant 60$ downstream of the $M10$ grid for both an injection pipe and nozzles were measured and compared. The results for an injection pipe showed that at any downstream location, the vertical profiles have about a 1.4 times greater half-width than those of the horizontal profiles, so an axisymmetric diffusion state could not be realized. This non-axisymmetric concentration field has appeared because three-dimensional disturbances were added to the flow field at the conduit and bending parts of the injection pipe, generating substantial inhomogeneity of turbulence. According to the diffusion theory of a fluid particle in three-dimensional space by Batchelor (1949), the degree of this inhomogeneity can be estimated as follows (see Sakai 1984 for details):

$$\frac{(\overline{v_3^2})^{\frac{1}{2}}}{(\overline{v_2^2})^{\frac{1}{2}}} \approx \frac{b_{\Gamma_z}}{b_{\Gamma_y}},$$

where v_2 and v_3 are Lagrangian velocities of a fluid particle in the y- and z-directions, respectively. Therefore, assuming that the difference in the mean concentration spread between the y- and z-directions was mainly caused by the inhomogeneity of the Lagrangian velocity field, the degree of inhomogeneity can be roughly estimated as $(\overline{v_3^2})^{\frac{1}{2}}/(\overline{v_2^2})^{\frac{1}{2}} \approx 1.43$. On the other hand, for nozzles, the difference in the spreads between the vertical and horizontal profiles were almost imperceptible, and good axisymmetric profiles were realized. Hence, it can be expected that the inhomogeneity of turbulence in the (y, z)-plane for nozzles is much smaller than for an injection pipe. It should be noted here that, although the sample matter was injected through a pipe inserted from the outside in the previous studies (Yamamoto & Sato 1979; Gad-el-Hak & Morton 1979), no comments were made on the axisymmetric characteristic of the mean-concentration field.

To estimate the turbulence production caused by the disturbance effect of nozzles on the velocity field, the representative term for the turbulent production in the turbulent energy equation is $\overline{u_x u_r}(\partial U_x/\partial r)$ because of axisymmetry of the velocity field downstream of the nozzle. If we represent the characteristic lengthscale of the disturbed area by l and the characteristic deficit velocity by ΔU, the production term may be estimated as $\overline{u_x u_r}(\partial U_x/\partial r) \approx \Delta U \overline{u_x^2}/l$. From the actual data at $x/M = 30$ in the case of the $M10$ grid, $l = 30$ mm and $\Delta U = 0.02 U_0$, and we also assume that $\overline{u_x^2}$ is comparable with the turbulence intensity out of the disturbed flow field. We can then estimate the value of the production term as $\overline{u_x u_r}/(\partial U_x/\partial r) \approx 2.02$ mm^2/s^3,

whereas from (2) the surrounding dissipation is $\epsilon \fallingdotseq 12.2\ \mathrm{mm^2/s^3}$. Thus, the turbulence production is fairly small compared with the dissipation in the surrounding flow field. Although it is very difficult to estimate accurately how this turbulence production has an influence on the diffusion process, since a self-propelled wake with no net momentum defect decays so much faster than a wake with a finite momentum defect (Tennekes & Lumley 1979, pp. 124–127), it can be expected that there is almost no serious disturbance by the nozzle wake of the present diffusion field in the region downstream of $13.5 \leqslant x/d_{\mathrm{N}}$.

On the basis of the above discussions, the method of introducing dye solution by nozzles was adopted here. The injection velocity of dye solution from the nozzle was about 1–1.5 times that of the main mean velocity; these velocities were selected so as to cancel the momentum loss due to the wakes of the nozzles. We could not avoid some variation of the injection velocity in each experiment owing to the change in the connecting rubber tube. But the degree of disturbance for the mean velocity by the wakes of the nozzles was always restricted to within 2.0% of the main velocity at $x/M = 3$. It should be noted that without an appropriate injection velocity, measurements precise enough to detect a stable concentration field are almost impossible. In the experiment by Gad-el-Hak & Morton (1979), the release velocity was 2.5 times as large as the main velocity.

3. Experimental results and discussion of the mean concentration field

3.1. *Experimental results*

The radial profile of the mean concentration for each grid is shown in figure 5, where Γ_{c} is the mean concentration on the plume axis and b_Γ is the half-width of the mean concentration profiles in the (x, z)-cross-section (hereafter b_Γ always indicates the half-width in the z-direction). In the figure, experimental data obtained at various downstream locations ($x/M = 26.5$, 30, 40, 50, 60, 70, 80 for the $M10$ grid and $x/M = 13.25$, 20, 25, 30, 35, 40 for the $M20$ grid) are plotted. It can be seen from this figure that, at $26.5 \leqslant x/M \leqslant 80$ and $13.25 \leqslant x/M \leqslant 40$ for the $M10$ and $M20$ grids, respectively, the mean concentration profiles have a similar shape described in terms of the following Gaussian function:

$$\frac{\Gamma}{\Gamma_{\mathrm{c}}} = \exp\{-(\ln 2)\,\eta^2\}, \quad \eta = \frac{r}{b_\Gamma}. \tag{5}$$

The solid lines in figure 5 represent Gaussian profiles from (5). Experimental results obtained are much less scattered and more reliable than other experimental data (for example, Gad-el-Hak & Morton 1979). Further, it should be noted here that the locations of the present sources ($x/M = 2$ and 1.5 for the $M10$ and $M20$ grids) are still in the inhomogeneous and developing region of turbulence just behind the grids. Hence, it could be supposed that the diffusion process of the plume at $x/M \leqslant 10$ has been influenced by the inhomogeneous turbulent field. However, the measuring regions of the present experiments ($26.5 \leqslant x/M \leqslant 80$ for $M10$ and $13.25 \leqslant x/M \leqslant 40$ for $M20$) are quite far downstream of the grids, and in these regions the turbulent statistics can be expected to be almost those for typical grid turbulence. Further, since the actual experimental results show a very good similarity, the diffusion mechanism of the plume in the far-downstream regions can be considered to have not been directly influenced by the developing stage of the plume just behind the grids.

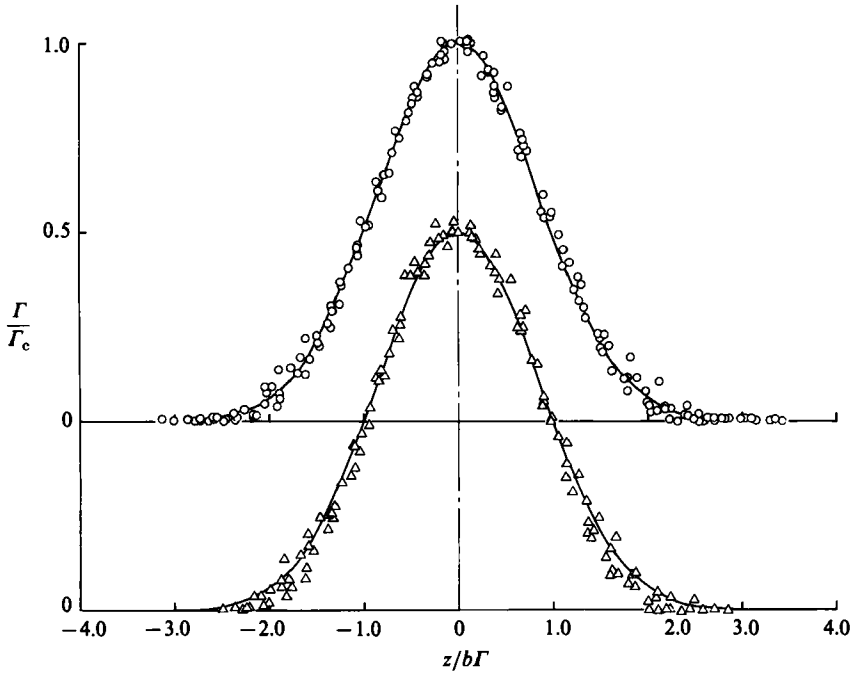

FIGURE 5. Radial profiles of non-dimensional mean concentration Γ/Γ_c. ○, $M = 10$ mm; △, $M = 20$ mm; ——, Gaussian curve.

Next we investigate the downstream evolution of the mean concentration field. According to Taylor's diffusion theory (for example, Hinze 1975, p. 435), the variation of variance of the mean concentration profile σ_Γ^2 for long diffusion times can be given as follows:

$$\sigma_\Gamma^2 = \frac{2D_T}{U_0}(x - x_0), \tag{6}$$

where x_0 is the x-coordinate of virtual origin for the spread of σ_Γ^2. Assuming that the mean concentration profiles have a similar Gaussian distribution to (5), b_Γ^2 can be related to σ_Γ^2 by

$$b_\Gamma^2 = 1.39\sigma_\Gamma^2. \tag{7}$$

Figure 6 shows the downstream variation of the squared half-width b_Γ^2 calculated by fitting the mean concentration profiles in the (x, z)-plane to Gaussian curves. Data are plotted on a logarithmic scale. The chain and solid lines in the figure are approximate lines obtained by assuming that the variation of b_Γ^2 obeys the 1-power law in the downstream direction for both grids. It can be seen that both lines represent well the variations of b_Γ^2 for both grids. This means that the present plume develops as a long-time dispersion. The values of turbulent diffusivity D_T calculated from the slopes of the spreads of σ_Γ^2 or b_Γ^2 are 6.50 mm²/s and 15.6 mm²/s for the $M10$ and $M20$ grids, respectively.

The downstream variation of b_Γ^2 normalized by D_T, M, U_0 on the basis of (6) and (7) are shown in figure 7, where the data are plotted on a linear scale. In adopting this normalization, the b_Γ^2 data can be rearranged on common straight lines.

The downstream variation of the reciprocal of the centreline mean concentration Γ_c, normalized by the mean concentration Γ_J at the nozzle exit, is shown in

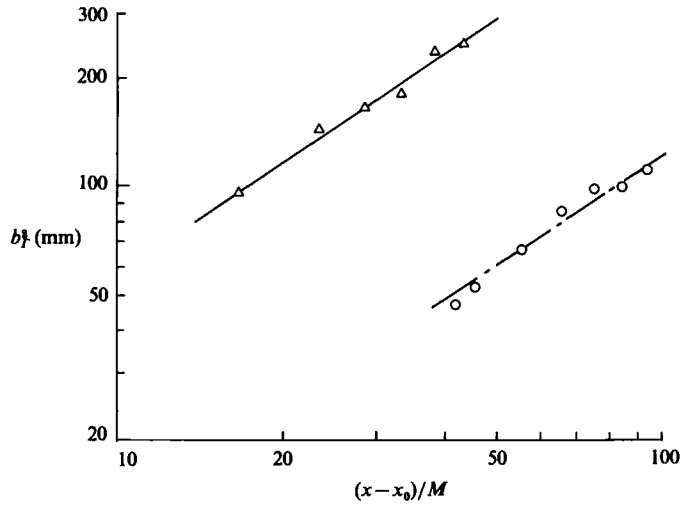

FIGURE 6. Downstream variation of the squared half-width $b_T^{\frac{1}{2}}$ for the mean concentration profile. ○, $M = 10$ mm; ——, $b_T^{\frac{1}{2}} = 5.80(x/M+3.61)$; △, $M = 20$ mm; – – –, $b_T^{\frac{1}{2}} = 1.21(x/M+15.5)$.

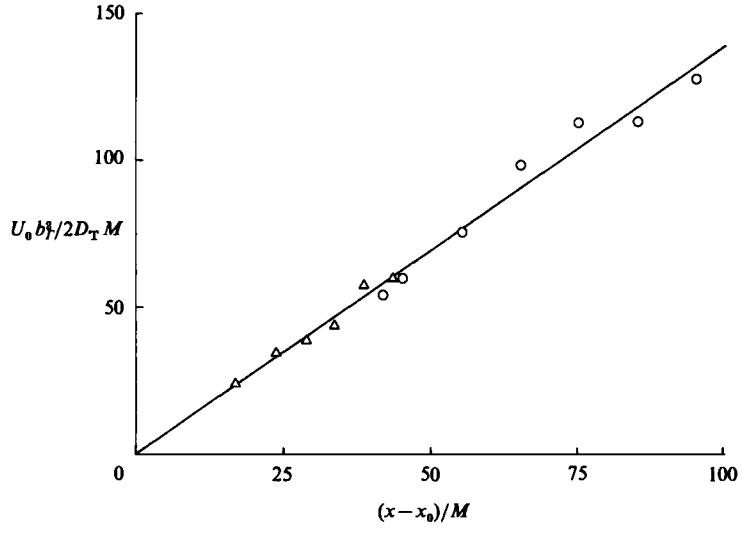

FIGURE 7. Downstream variation of $U_0 b_T^{\frac{1}{2}}/2D_T M$. ○, $M = 10$ mm; △, $M = 20$ mm; ——, $U_0 b_T^{\frac{1}{2}}/(2D_T M) = 1.39(x-x_0)/M$.

figure 8. It is found that Γ_c obeys well the hyperbolic decay law for both grids. The data can be fitted to the following function:

$$\frac{\Gamma_J}{\Gamma_c} = k_1\left(\frac{x}{M-a_1}\right), \tag{8}$$

as shown on the figure.

These experimental results, especially the variations of $b_T^{\frac{1}{2}}$ and Γ_c in figures 7 and 8, suggest that the effects of the disturbances induced by a nozzle body on the concentration field are not serious.

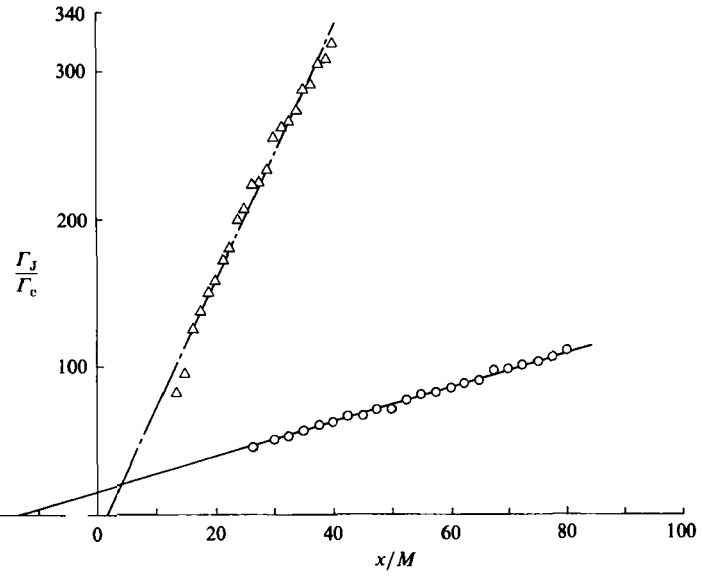

FIGURE 8. Downstream variation of non-dimensional reciprocal mean concentration Γ_J/Γ_c on the plume axis. ○, $M = 10$ mm; ——, (8) with $k_1 = 1.19$, $a_1 = -12.9$; △, $M = 20$ mm; – – –, (8) with $k_1 = 8.59$, $a_1 = 1.72$.

3.2. *Similarity of the mean concentration field*

An analysis of the mean concentration field for the present case can be given by superposition of the solution for an instantaneous point source (see Carslaw & Jaeger 1959, p. 266). Here, a more concise method will be used, applying a thin-layer approximation to the mean concentration equation and the turbulent-diffusivity concept of matter. Neglecting the effect of molecular diffusivity, the fundamental equation for the problem is as follows:

$$U_0 \frac{\partial \Gamma}{\partial x} = \frac{1}{r} \frac{\partial}{\partial r}[r(-\overline{\gamma u_r})], \tag{9}$$

where u_r is the velocity fluctuation in the r-direction. Using the non-dimensional coordinates defined by $\xi = x/M$, $\eta = r/b_\Gamma$, the following similar functions $f(\eta)$, $g(\eta)$ are assumed:

$$\Gamma(\xi, \eta) = \Gamma_c(\xi) f(\eta), \quad -\overline{\gamma u_r} = a_0(\xi)\, g(\eta).$$

Also assumed is the gradient type of diffusion model

$$-\overline{\gamma u_r} = D_T \frac{\partial \Gamma}{\partial r}. \tag{10}$$

Integration of (9) with respect to r gives $2\pi \int_0^\infty r\Gamma U_0 \, \mathrm{d}r = \text{const.} = H$. From the similarity assumption, this equation reduces to

where

$$\left.\begin{aligned} \Gamma_c b_r^2 &= \frac{H^*}{U_0}, \\ H^* &= \frac{H}{2\pi \int_0^\infty \eta f \, \mathrm{d}\eta}. \end{aligned}\right\} \tag{11}$$

From the above discussion, (9) becomes

$$\frac{1}{2}\frac{U_0}{M}\frac{\mathrm{d}b_\Gamma^2}{\mathrm{d}\xi}\eta f + D_\mathrm{T}\frac{\mathrm{d}f}{\mathrm{d}\eta} = 0. \tag{12}$$

The condition of similarity requires that the coefficient multiplied by ηf in (12) should be a constant, if D_T is a function of η alone. Consequently,

$$\frac{1}{2}\frac{U_0}{M}\frac{\mathrm{d}b_\Gamma^2}{\mathrm{d}\xi} = \text{const}, \quad \text{so } b_\Gamma^2 \propto \xi. \tag{13}$$

Equation (13) means that b_Γ^2 increases linearly in the downstream direction. It can be found from (11) and (13) that Γ_c obeys a hyperbolic decay law.

When D_T = constant, the solution of (12) can be expressed as follows:

$$f(\eta) = \exp(-P\eta^2), \quad P = \frac{U_0(\mathrm{d}b_\Gamma^2/\mathrm{d}\xi)}{4MD_\mathrm{T}} = \ln 2, \tag{14}$$

where the boundary condition $f(0) = 1$ was used. Equation (14) means that a similar solution is a Gaussian distribution. The result obtained is the same as an approximate solution (Hinze 1975, p. 428) for the three-dimensional diffusion problem from a continuous point source in a uniform flow. From (14), the turbulent diffusivity D_T is given by

$$D_\mathrm{T} = \frac{U_0}{4M\ln 2}\frac{\mathrm{d}b_\Gamma^2}{\mathrm{d}\xi}. \tag{15}$$

The value of D_T in the discussion of figure 6 were calculated by (15). By substituting b_Γ^2 obtained by integrating (15) and $H = \frac{1}{4}\pi d_\mathrm{N}^2 U_\mathrm{J}\Gamma_\mathrm{J}$ into (11) and using (14) for $f(\eta)$, concerning the decay of Γ_c, (8) can be obtained. In (8), the constant k_1 is $k_1 = 16D_\mathrm{T}/d_\mathrm{N}^2 U_\mathrm{J}$, and the location of the virtual origin x_0 was adjusted for the variation of (8) to fit the data of Γ_c.

Assuming a similar mean concentration profile, integration of (9) yields

$$-\overline{\gamma u_r} = a_0(\xi)\,g(\eta) = -\frac{\Gamma_\mathrm{c}\,U_0(\mathrm{d}b_\Gamma/\mathrm{d}\xi)}{M}\eta f(\eta). \tag{16}$$

It is easy to predict the profile of $-\overline{\gamma u_r}$ by substituting the Gaussian curve (14) for $f(\eta)$. Although the experimental results for $\overline{\gamma u_r}$ were given by Gad-el-Hak & Morton (1979), their data are too scattered to compare with the above predicted profile. Further, the profile of the advection term in the mean-concentration equation (9) can be also predicted by assuming the Gaussian curve for $f(\eta)$. As a result, it could be shown that in the core region of the concentration field, the advection term gives the gain of the mean concentration, and in the outer region it indicates the loss. The diffusion term always counterbalances the advection term.

4. Experimental results on the fluctuating concentration field

A detailed discussion of the characteristics of the fluctuating concentration field will be given in §§5 and 6. Figure 9 shows a record of the output signal near the central part ($z/b_\Gamma = 0.102$) of the concentration field at $x/M = 26.5$ for the $M10$ grid. In the figure, one can distinguish clearly the detecting part (part A) and non-detecting part (part B) of the concentration, showing that the signal obtained is fairly intermittent even in the core region of the concentration field. This result is remarkably different from the data by Gad-el-Hak & Morton (1979) which showed that the intermittency

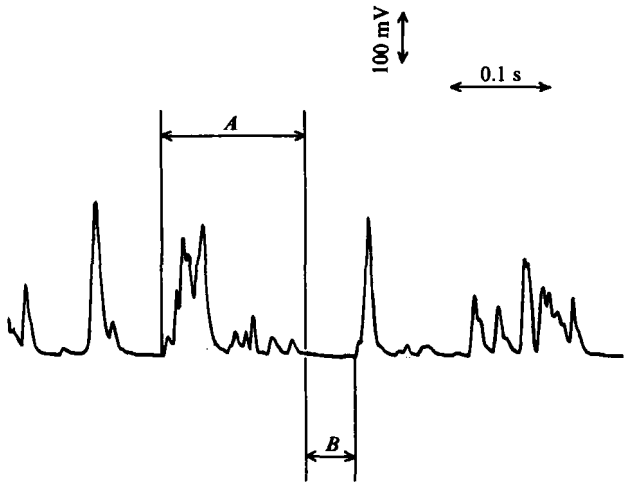

FIGURE 9. An example of output signal of the concentration measuring system for $x/M = 26.5$, $M = 10$ mm, $z/b_\Gamma = 0.102$ and $\Gamma_j = 3.0$ g/l. *A*, periods in the fluctuating concentration field; *B*, periods without the concentration fluctuation.

factor for the concentration field takes an almost constant value of 1.0 in the core region.

The radial profiles of the non-dimensional concentration fluctuation r.m.s. values γ'/γ'_c for the grids of $M10$ and $M20$ are shown in figure 10, where γ'_c indicates the r.m.s. value on the centreline. In the figure, experimental data obtained at various locations are plotted as for the mean concentration profiles in figure 5, with the same measuring locations. As shown in the figure, the radial profiles of γ'/γ'_c are nearly similar for both grids. The solid and chain lines in figure 10 indicate similar solutions for the respective grids $M10$ and $M20$, which will be discussed in §5.

Figure 11 shows the radial profiles of the ratio of the concentration fluctuation r.m.s. value γ' to the mean concentration Γ. The meaning of the symbols in the figure are the same as in figure 10. It can be seen that as a whole, the profiles for both grids seem to be nearly similar. Here, it should be noted that the values of γ'/Γ on the centreline are over 1.0, since the concentration-fluctuation signals are rather intermittent as shown in figure 9.

Figure 12 shows the downstream variation of $U_0 b_{\gamma'}^2/2D_T M$, which was obtained by non-dimensionalizing the half-width $b_{\gamma'}$ for the radial profiles of γ'/γ'_c by using D_T, U_0 and M. The values of $U_0 b_{\gamma'}^2/2D_T M$ for both grids collapse on a common straight line described by

$$\frac{U_0 b_{\gamma'}^2}{2D_T M} = 2.86\left(\frac{x-x_0}{M}\right), \tag{17}$$

where $x_0 = -15.4M$ for $M10$ and $x_0 = 3.61M$ for $M20$, and these values are the same as the virtual origins for the spread of b_Γ^2. Calculating the ratio of $b_{\gamma'}$ to b_Γ from (6), (7) and (17), we obtain $b_{\gamma'}/b_\Gamma = (2.86/1.39)^{\frac{1}{2}} = 1.43$.

Figure 13 shows the downstream variations of Γ_J/γ'_c, where Γ_J is the mean concentration at the release source. The variation of γ'_c for both grids obeys well the hyperbolic decay law described by

$$\frac{\Gamma_J}{\gamma'_c} = k_2\left(\frac{x}{M} - a_2\right), \tag{18}$$

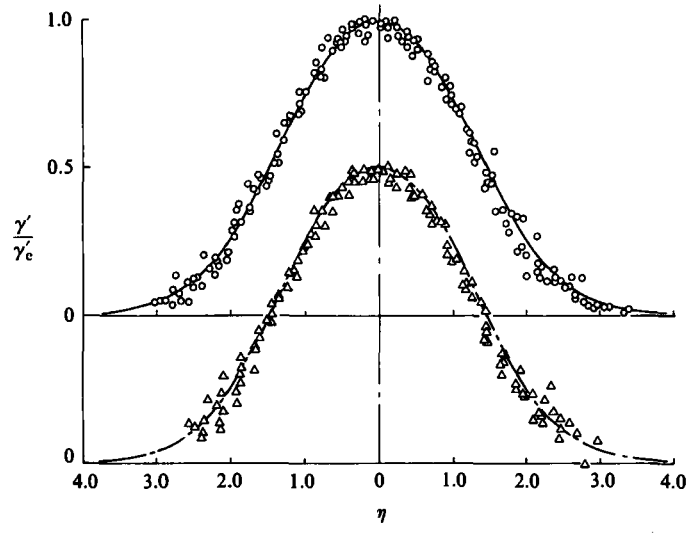

FIGURE 10. Comparison between experimental results and calculated profile for γ'/γ'_c. ○, experimental results ($M = 10$ mm); ——, similar solution ($\gamma'_c/\Gamma_c = 1.6$, $D_T/A_T = 1.0$); △, experimental results ($M = 20$ mm); – – –, similar solution ($\gamma'_c/\Gamma_c = 1.3$, $D_T/A_T = 1.0$).

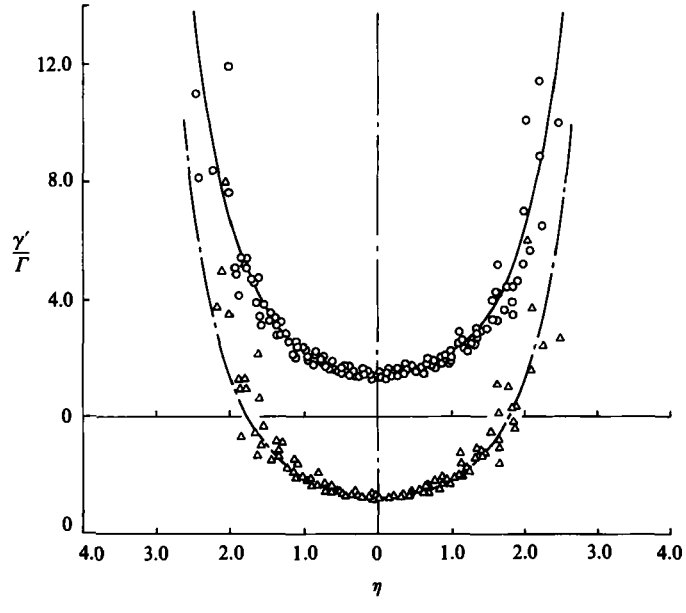

FIGURE 11. Comparison between experimental results and calculated radial profile, for γ'/Γ. ○, experimental results ($M = 10$ mm); ——, similar solution ($\gamma'_c/\Gamma_c = 1.6$, $D_T/A_T = 1.0$); △, experimental results ($M = 20$ mm); – – –, similar solution ($\gamma'_c/\Gamma_c = 1.3$, $D_T/A_T = 1.0$).

as shown on the figure. It should be noted here that a rather large difference between the values of k_2 for the $M10$ and $M20$ grids has appeared. The reasons for this will be discussed later in connection with the downstream variation of the relative intensity shown in the next figure.

Figure 14 shows the variation of the ratio of γ'_c to Γ_c on the centreline of the

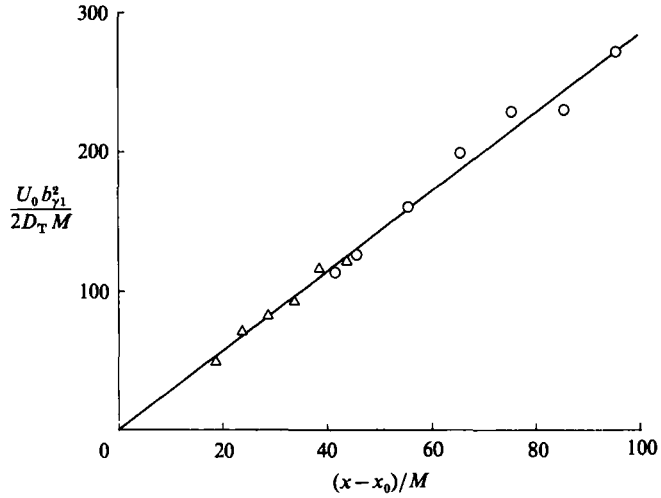

FIGURE 12. Downstream variation of squared half-width b_{γ}^2, for the radial profile of γ'/γ_c'. ○, $M = 10$ mm; △, $M = 20$, mm; ——, $U_0 b_{\gamma}^2/2D_T M = 2.86(x-x_0)/M$.

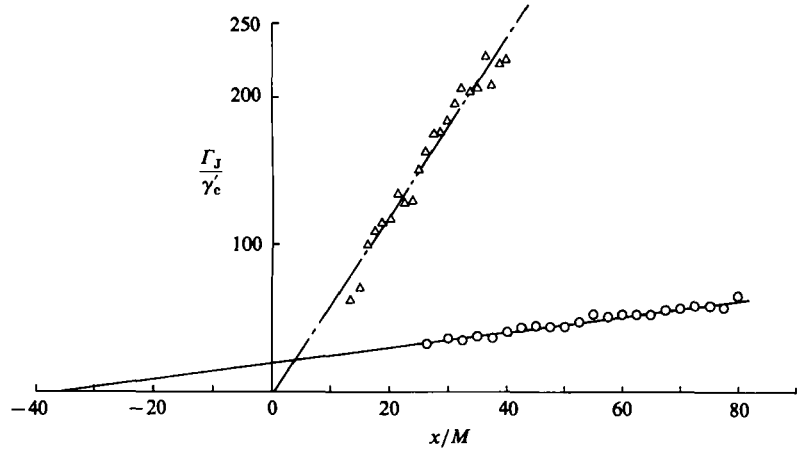

FIGURE 13. Downstream variation of non-dimensional reciprocal r.m.s. value Γ_J/γ_c' on the plume axis. ○, $M = 10$ mm; △, $M = 20$ mm; ——, (18) with $k_2 = 0.546$, $a_2 = -35.1$; – –, (18) with $k_2 = 6.08$, $a_2 = 0.470$.

concentration fields. γ_c'/Γ_c shows a gradual increase downstream for both grids. These variations of γ_c'/Γ_c can be predicted from (8) and (18), which becomes as follows:

$$\frac{\gamma_c'}{\Gamma} = k_1\left(\frac{x}{M}-a_1\right)\Big/\left\{k_2\left(\frac{x}{M}-a_2\right)\right\}. \tag{19}$$

The prediction using (19) are shown on figure 14.

Here, the difference of the values of k_2 between the $M10$ and $M20$ grids will be examined by considering the relationship among k_1, k_2 and γ_c'/Γ_c. k_2 is related to k_1 and γ_c'/Γ_c through the empirical equation (19). γ_c'/Γ_c had values of 1.4–1.7 and 1.3–1.4 for $M10$ and $M20$, respectively. These values seem to be reasonable on account of the intermittency in the core region of the concentration field (see figure 9). On the other hand, the values of k_1 were 1.19 for the $M10$ grid and 8.59 for $M20$ grid,

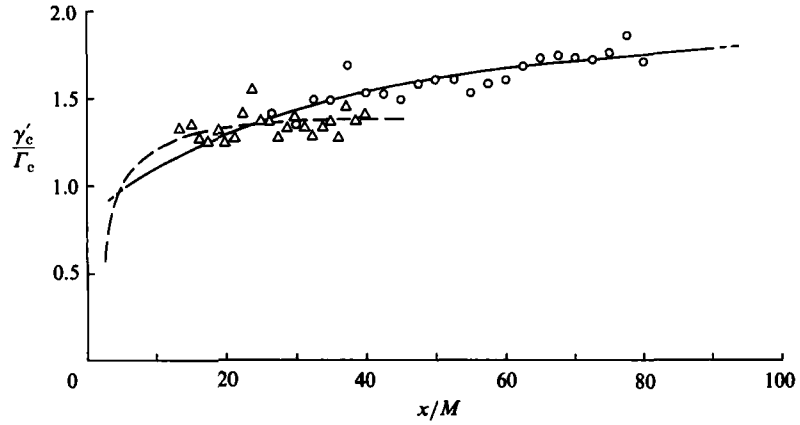

FIGURE 14. Downstream variation of γ_c'/Γ_c on the centreline. ○, $M = 10$ mm; ——, (19) with $k_1 = 1.19$, $a_1 = -12.9$, $k_2 = 0.546$, $a_2 = -35.1$; △, $M = 20$ mm; – – –, (19) with $k_1 = 8.59$, $a_1 = 1.72$, $k_2 = 6.08$, $a_2 = 0.470$.

which is a significant difference. However, since k_1 is determined by the experimental conditions of D_T, M, d_N and U_J through the equation $k_1 = 16 D_T M/d_N U_J$ given in §3.2, it is not surprising that this degree of difference between the values of k_1 for both grids has appeared. From (19), it is easily understood that these experimental values of γ_c'/Γ_c and k_1 lead to the rather large difference of k_2 mentioned earlier. It is worth noting that the experimental condition have a great influence on the quantitative decay rate of the concentration-fluctuation r.m.s. value in this way.

5. Similarity of the fluctuating concentration field

The equation for the concentration fluctuation intensity $\overline{\gamma^2}$, using a thin-layer approximation, can be described as follows (Csanady 1980):

$$U_0 \frac{\partial \overline{\gamma^2}}{\partial x} = -2\overline{\gamma u_r}\frac{\partial \Gamma}{\partial r} - \frac{1}{r}\frac{\partial}{\partial r}(r\overline{\gamma^2 u_r}) - \chi, \tag{20}$$

where χ is the dissipation term of $\overline{\gamma^2}$ due to the molecular diffusion ($= 2D_m\overline{(\partial\gamma/\partial x_i)^2}$). $-\overline{\gamma u_r}$, $-\overline{\gamma^2 u_r}$, and χ are assumed to be of the forms

$$-\overline{\gamma u_r} = D_T \frac{\partial \Gamma}{\partial r}, \quad -\overline{\gamma^2 u_r} = A_T \frac{\partial \overline{\gamma^2}}{\partial r},$$

$$\chi = 2D_m\left(\frac{\partial \gamma}{\partial x_i}\right)^2 = 12 D_m \overline{\gamma^2}/\lambda_\gamma^2,$$

where D_T, A_T are the eddy diffusivities for the mean concentration and fluctuation intensity, and λ_γ represents the dissipation scale for the $\overline{\gamma^2}$ field. As usual, the following similar forms of Γ and $\overline{\gamma^2}$ are assumed: $\Gamma(\xi, \eta) = \Gamma_c(\xi) f(\eta)$, $\overline{\gamma^2}(\xi, \eta) = b_c(\xi)\, h(\eta)$, where $\xi = x/M$, $\eta = r/b_\Gamma$. With the above assumptions and (11), (14) and (15) for the mean concentration field, the following ordinary differential equation for $h(\eta)$ can be obtained from (20):

$$\frac{d^2h}{d\eta^2} + \left(\frac{1}{\eta} + C\frac{D_T}{A_T}\eta\right)\frac{dh}{d\eta} + \left(4C\frac{D_T}{A_T} - \alpha h\right) = -2\frac{D_T}{A_T}\frac{\Gamma_c^2}{b_c}C^2\eta^2 \exp(-C\eta^2), \tag{21}$$

where $C = \ln 4$, $\alpha = 12 D_m b_\Gamma^2 / \lambda_\gamma^2 A_T$. The parameters are A_T/D_T, b_c/Γ_c^2 and α. The boundary conditions are

$$\eta = 0; \quad \frac{dh}{d\eta} = 0, \quad \eta \to \infty; \quad h \to 0. \tag{22a, b}$$

Equation (21) has the following series solution;

$$h(\eta) = \sum_{n=0}^{\infty} a_{2n} \eta^{2n}, \tag{23}$$

where

$$\left.\begin{aligned} a_0 &= 1, \quad a_2 = \frac{1}{4}\left\{\alpha - C\frac{D_T}{A_T}\right\} a_0, \\ a_{2n} &= \frac{\alpha - 2(n+1) C D_T/A_T}{4n^2} a_{2n-1} - \frac{(D_T/A_T)(\Gamma_c^2/b_c) C^2 (-C)^{n-2}}{2n^2 (n-2)!} \quad (n \geqslant 2). \end{aligned}\right\} \tag{24}$$

Equation (23) has only even powers of η because of the evident symmetry. Although the similarity equation (21) is essentially equivalent to that derived by Csanady (1967), the latter investigator did not make a comparison with any grid-turbulence experiments.

The condition of similarity requires the constancy of coefficients in (21). When D_T and A_T are constant, the following decay laws concerning $b_c(\xi)$, λ_γ^2 are obtained:

$$b_c(\xi) \propto \xi^{-2}, \quad \lambda_\lambda^2 \propto \xi, \tag{25a, b}$$

since $b_\Gamma^2 \propto \xi$, $\Gamma \propto \xi^{-1}$ (see §3.2). Consequently, the r.m.s. value of fluctuating concentration on the axis γ_c' decays as a hyperbola in the downstream direction, while λ_γ^2 develops linearly. The experimental results show this property of γ_c', unnoticed by Csanady (1967), as shown in figure 13.

In the actual calculations, D_T/A_T and b_c/Γ_c^2 are fixed and the remaining parameter α is selected for the solution to satisfy the outer boundary condition by a shooting method.

In figures 10 and 11, similar profiles calculated for γ'/γ_c' and γ'/Γ are included with the experimental data. For the radial profile of the mean concentration, the Gaussian curve of (14) was used. In the figures, parameters for the calculation are $\gamma_c'/\Gamma_c = 1.6$, $D_T/A_T = 1.0$, and $\alpha = 3.29$ for the $M10$ flow and $\gamma_c'/\Gamma_c = 1.3$, $D_T/A_T = 1.0$ and $\alpha = 3.53$ for the $M20$ flow. Although there is excellent agreement between the theoretical similar profiles and experiments for both γ'/γ_c' and γ'/Γ, it should be noted that two different groups of parameters are needed to obtain a coincidence each of $M10$ and $M20$. The exact similarity indicates that these parameters must constitute only one group. The present results suggest that the fluctuating concentration field has only an approximate similarity. A plausible explanation of this approximate similarity will be ascribed to the difference of grid Reynolds number for each mesh. The agreement between the theory and experiment was obtained by putting $D_T/A_T = 1.0$, which means the equivalence of each coefficient for two gradient diffusion models of transport terms $-\overline{\gamma u_r}$ and $-\overline{\gamma^2 u_r}$. Csanady (1967) assumed this equivalence and compared his calculation with the experiment of Becker *et al.* (1966), in which oil smoke was released in a fully developed pipe flow. Agreement was not sufficient for that comparison.

6. Consideration of the fluctuating concentration signal by a random rectangular-wave model

In order to investigate the diffusion process of the scalar quantity in turbulent flows, Uberoi & Corrsin (1953) conducted an analysis of the thermal diffusion from a heated line source in grid-generated turbulent flow, assuming that the fluctuating temperature signal is represented by a randomly spaced sequence of rectangular pulses of constant height and width. This study is an extension of their investigation, providing an analysis of the fluctuating concentration field by approximating the fluctuating concentration signal to a randomly spaced sequence of rectangular waves with various heights and widths.

Figure 15 shows a conceptual diagram of the diffusion process in the grid-generated turbulence and an example of the approximated fluctuating concentration signal. The transport of the diffusing matter released from the continuous point source by the moving fluid particles leads to the situation in which a substantial volume first occupied by diffusing matter is elongated in one direction and compressed in another to form highly distorted layers, twisted lines and deformed lumps. In the case of negligible molecular diffusion, the fluctuating concentration signal observed at a fixed point Q can be expected to become a randomly spaced sequence of rectangular waves, which have a constant concentration during the passage of the layers, lines or lumps through the point Q and zero concentration after passing. But the larger the effect of molecular diffusion, the more variable the concentration; the concentration signals detected are no longer rectangular. Hereupon, it is assumed that each concentration signal does not have a constant height but still remains rectangular. This assumption corresponds to the partial modelling of molecular diffusion. It should be noticed here that the variation in the height of each concentration signal can be caused not only by the effect of molecular diffusion but also by the inevitable situation in which a sampling volume of the light probe is not small enough compared with the size of a marked particle of diffusion matter.

Considering the above assumptions, it can be expected that the variation process of the concentration signal detected at a point Q becomes like figure 15(*b*). As shown in figure 15(*b*), t_i is the time when the ith jump in the height of rectangular waves counted from $t = 0$ has occurred. A_i is the height of the rectangular wave at that time and $|J_i|$ is the length of time during which the height A_i is maintained. (Here, a symbol $|\,|$ does not indicate an absolute value but a duration of the height A_i.) Further, t_{i+1} denotes the time when the next jump of the height has occurred. Defining J_i as follows:

$$J_i(t) = \begin{cases} 1 & t_i \leqslant t \leqslant t_{i+1}, \\ 0 & \text{for all other } t, \end{cases} \tag{26}$$

the whole process of the concentration signals can be described by

$$\tilde{\Gamma}(t) = A_1 J_1(t) + A_2 J_2(t) + \ldots + A_i J_i(t) + \ldots. \tag{27}$$

For an observing time T_t long enough, the mean concentration Γ is given by

$$\Gamma = \frac{1}{T_t}\int_0^\infty \tilde{\Gamma}(t)\,\mathrm{d}t = \frac{1}{T_t}\sum_i A_i|J_i|. \tag{28}$$

Therefore, the mean-square value for the concentration fluctuation $\overline{\gamma^2}$ becomes

$$\overline{\gamma^2} = \frac{1}{T_t}\int_0^\infty \{(\sum_i A_i J_i(t))(\sum_j A_j J_j(t)) - 2\Gamma\sum_i A_i J_i(t) + \Gamma^2\}\,\mathrm{d}t = \frac{\sum_i A_i^2|J_i| - \Gamma^2 T_t}{T_t}, \tag{29}$$

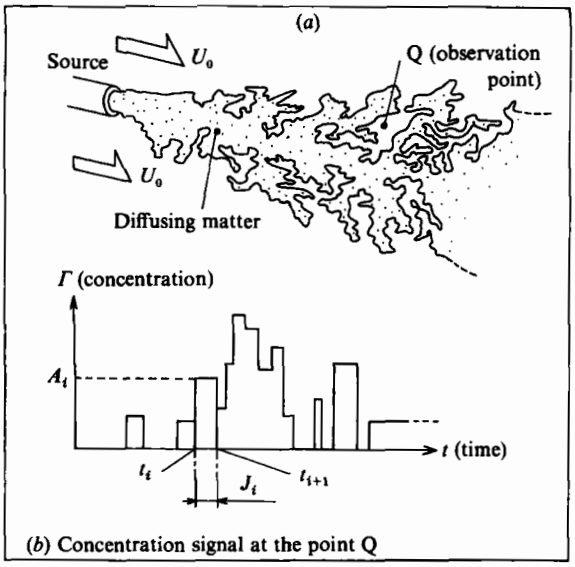

FIGURE 15. (*a*) Diagram of the diffusion state of matter in the grid-generated turbulence and (*b*) an example of the approximated fluctuating concentration signal.

where $J_i J_j = 0$ for $i \neq j$, and $J_i J_i = 1$. Since $\Gamma T_t = \sum_i A_i |J_i|$, γ'/Γ should be given by

$$\frac{\gamma'}{\Gamma} = \left[\frac{\sum_i A_i^2 |J_i| - \Gamma^2 T_t}{T_t}\right]^{\frac{1}{2}} \Big/ \frac{\sum_i A_i |J_i|}{T_t} = \left(\frac{\Gamma_c}{\Gamma} P - 1\right)^{\frac{1}{2}}, \quad P = \frac{1}{\Gamma_c} \frac{\sum_i A_i^2 |J_i|}{\sum_i A_i |J_i|}. \tag{30}$$

For the model of Uberoi & Corrsin (1953), A_i is constant. From (30) with $A_i = \text{const} = A$, we can obtain $P = A/\Gamma_c$, which means that P is the ratio of the height of the rectangular wave to the mean concentration on the plume axis.

Assuming (5), the following equations can be obtained from (30):

$$\frac{\gamma'}{\Gamma_c} = \frac{\gamma'}{\Gamma} \exp(-\eta^2 \ln 2), \tag{31a}$$

$$\frac{\gamma'}{\gamma'_c} = \frac{\Gamma_c}{\gamma'_c} \frac{\gamma'}{\Gamma} \exp(-\eta^2 \ln 2), \tag{31b}$$

$$\frac{\gamma'}{\Gamma} = [P \exp(\eta^2 \ln 2) - 1]^{\frac{1}{2}}. \tag{31c}$$

From the variation of radial profiles for γ'/Γ_c, γ'/γ'_c and γ'/Γ with the parameter P, it can be found that for $P < 2$, the peaks for the profiles of γ'/Γ_c and γ'/γ'_c have not appeared on the centreline. For $P < 2$, which corresponds to $\alpha > 4(D_T/A_T) \ln 4$, the peaks have appeared in the similar solution of γ'/γ'_c at radial locations $\eta \neq 0$. The condition for this peak shift can be obtained easily from (23) and (24) by requiring $\mathrm{d}^2 h/\mathrm{d}\eta^2|_{\eta=0} > 0$. Next, the physical significance of α and the relationship between P and α will be considered qualitatively.

Since $\alpha = 12 D_m b_\Gamma^2/\lambda_\gamma^2 A_T$, situations with large α-values arise when λ_γ, A_T are small in comparison with D_m, b_Γ^2, that is when the dissipation lengthscale λ_γ for the concentration fluctuation has a small value and the turbulent diffusion of the concentration fluctuation intensity γ^2 is weak. In this case, it can be expected that

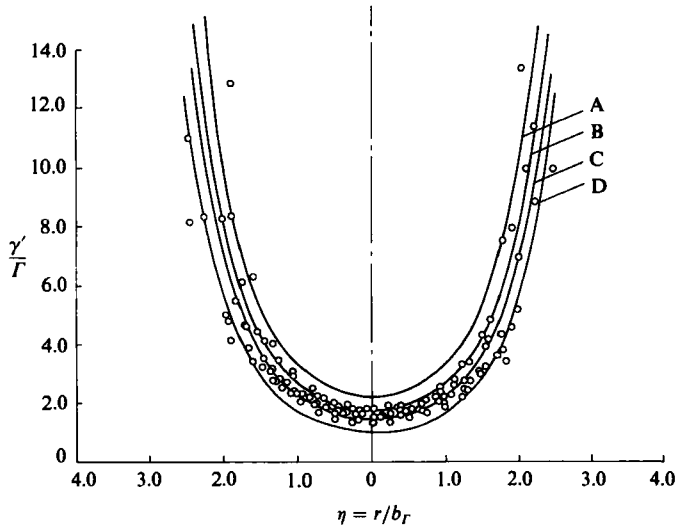

FIGURE 16. Comparison between radial profiles of γ'/Γ calculated by a random rectangular wave model and experimental results: ○, experimental results ($M = 10$ mm); A, (31) with $P = 6$, $\gamma'/\Gamma_c = 2.24$; B, (31) with $P = 4$, $\gamma'/\Gamma_c = 1.73$; C, (31) with $P = 3$, $\gamma'/\Gamma_c = 1.41$; D, (31) with $P = 2$, $\gamma'/\Gamma_c = 1.00$.

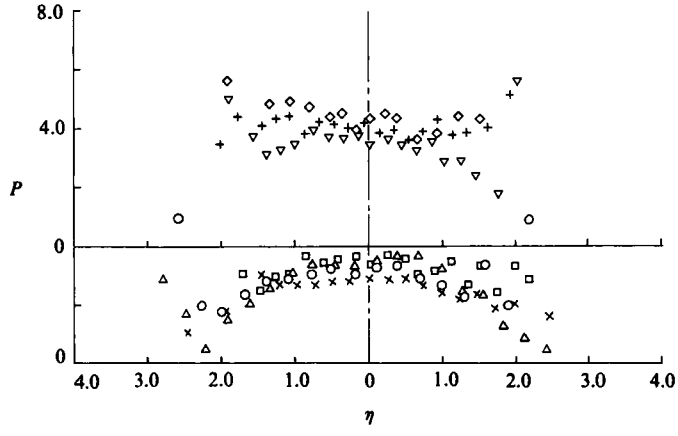

FIGURE 17. Radial profiles of parameter P ($M = 10$ mm: ○, $x/M = 26.5$; △, 30; ×, 40; □, 50; ▽, 60; +, 70; ◇, 80.

diffusing matter is not so extensive, but is distorted finely in a relatively narrow space, so that the fluctuating concentration signals become those with relatively small $|J_i|$ at short time intervals. Then the values of P will become smaller than the case in which the time intervals between rectangular waves are large. It should be noted that the radial profiles for γ'/Γ_c and γ'/γ'_c with $P < 1$ cannot exist because of the relation between γ'/Γ_c and P (i.e. $\gamma'_c/\Gamma_c = (P-1)^{\frac{1}{2}}$). In figure 16, a comparison is given between the experimental results for γ'/Γ and theoretical curves calculated using (31*c*) for grid $M10$. It can be seen from this figure that the calculated curves with $P = 3$–4 are in good agreement with the experimental results, although the assumptions used are very simple.

The profiles of P are shown in figures 17 and 18, for $M10$ and $M20$ respectively,

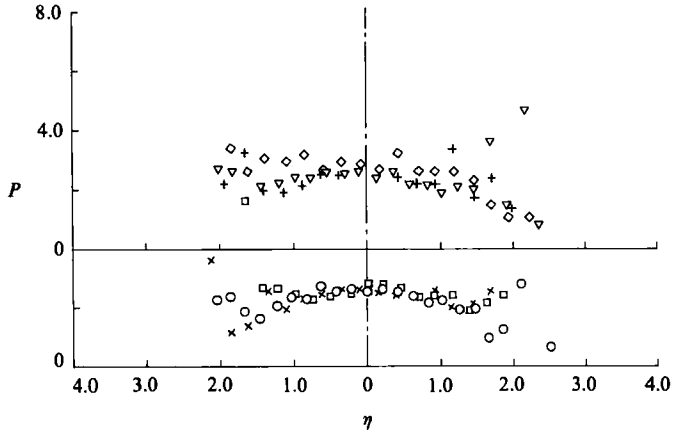

FIGURE 18. Radial profiles of parameter P ($M = 20$ mm): ○, $x/M = 13.25$; ×, 20; □, 25; ▽, 30; +, 35; ◇, 40.

where the values of P are calculated from (31c) using the experimental results for γ'/Γ. It is found from these figures that in the case of $M10$, the parameter P tends to increase in the downstream direction. The values are estimated as follows: $P = 3.3$ for $26.5 \leqslant x/M \leqslant 50$ and $P = 4.0$ for $60 \leqslant x/M \leqslant 80$, whereas in the case of $M20$, P does not change so much for $13.25 \leqslant x/M \leqslant 40$ and can be estimated to be about 2.6. Because there is a one-to-one correspondence between P and γ_c'/Γ_c, the increase of P for the $M10$ grid corresponds to the increase of the relative intensity γ_c'/Γ_c in figure 14.

7. Conclusions

The turbulent diffusion process has been examined in the case of a non-buoyant plume in grid-generated water turbulence. The grids used were biplane circular rods with mesh sizes 10 and 20 mm. The diffusing matter was dye solution, and the mean and fluctuating concentration fields were detected by the light-absorption method. Measurements have been made up to 800 mm downstream of the grids. When diffusion experiments from a continuous point source are actually conducted in grid-generated turbulence, a difficulty derives from the fact that the method of injecting dye solution into the flow field has a large influence on the concentration field. In this study, by using nozzles which were designed to disturb the flow field as little as possible, an almost axisymmetric concentration field could be realized. Experimental results obtained for the mean concentration and concentration fluctuation field were much less scattered and more reliable than previous data. From considerations of similarity for the thin-layer-approximated diffusion equation of the mean concentration Γ, the linear increase law of b_Γ^2 and the hyperbolic decay law of Γ_c were deduced, and they have been confirmed by the present experimental results. Concerning the radial mean concentration profiles, a Gaussian distribution could be obtained as a similar solution of the thin-layer-approximated diffusion equation for Γ, and it showed very good agreement with the experimental data. For both grids $M10$ and $M20$, radial profiles of the fluctuation r.m.s. value γ' and the ratio of γ' to mean concentration Γ become almost similar. The downstream variation of the centreline r.m.s. values γ_c' is in good conformity with a hyperbolic decay law, and γ_c'/Γ_c on the centreline tends to increase slightly in the downstream direction. In the

fluctuating concentration field, the similarity was found to be only approximately valid, and was derived on the basis of a gradient-type diffusion model for $\overline{\gamma^2 u_r}$ and $\overline{\gamma u_r}$ and an isotropic dissipation model. By selecting proper parameters of α, γ_c'/Γ_c and D_T/A_T for each $M10$ and $M20$ experiment, it is possible to make the similar solution of γ'/γ_c' agree with experimental data. Further, the fluctuating concentration field can be well described by approximating the fluctuating concentration signal with a randomly spaced sequence of rectangular waves having various heights and widths.

We would like to express our deep appreciation to Mr Tsuneo Suzuki of Toshiba Inc. for his generous and able assistance, to Mr Takehiro Kushida and Mr Hirokuni Kanda of the Mechanical Engineering Department of Nagoya University for their technical assistance, and to Miss Shiho Takagi of the Graphic Science Department of Nagoya University for her tracing of figures. The authors also wish to acknowledge the constructive criticism of the referees.

REFERENCES

ANAND, M. S. & POPE, S. B. 1983 Diffusion behind a line source in grid turbulence. In *Proc. 4th Symp. on Turbulent Shear Flows, Karlsrule Germany*, pp. 46–61. Springer.

BALDWIN, L. V. & MICKELSEN, W. R. 1962 Turbulent diffusion and anemometer measurements. *Proc. Am. Soc. Civ. Engrs* **88**, 37–69.

BATCHELOR, G. K. 1949 Diffusion in a field of homogeneous turbulence. *Austral. J. Sci. Res.* **2**, 437–450.

BATCHELOR, G. K. 1952 Diffusion in a field of homogeneous turbulence, the relative motion of particles. *Proc. Camb. Phil. Soc.* **48**, 345–362.

BATCHELOR, G. K. & TOWNSEND, A. A. 1948 Decay of isotropic turbulence in the initial period. *Proc. R. Soc. Lond.* A **193**, 539–558.

BATCHELOR, G. K. & TOWNSEND, A. A. 1956 Turbulent diffusion. In *Surveys in Mechanics*, pp. 352–399. Cambridge University Press.

BECKER, H. A., ROSENSWEIG, R. E. & GWOZDZ, J. R. 1966 Turbulent dispersion in a pipe flow. *AIChE J.* **12**, 964–972.

BIRCH, A. D., BROWN, D. R., DODSON, M. G. & THOMAS, J. R. 1978 The turbulent concentration field of a methane jet. *J. Fluid Mech.* **88**, 431–449.

BELORGEY, M., NGUYEN, A. D. & TRINITE, M. 1979 Diffusion from a line source in a turbulent boundary layer with transfer to the wall. In *Proc. 2nd Symp. on Turbulent Shear Flows, Imperial College, London*, pp. 129–142. Springer.

BRITTER, R. E., HUNT, J. C. R., MARSH, G. L. & SNYDER, W. H. 1983 The effects of stable stratification on turbulent diffusion and the decay of grid turbulence. *J. Fluid Mech.* **127**, 27–44.

CARSLAW, H. S. & JAEGER, J. C. 1959 *Conduction of Heat in Solids*, p. 266. Oxford University Press.

COMTE-BELLOT, G. & CORRSIN, S. 1966 The use of a contraction to improve the isotropy of grid-generated turbulence. *J. Fluid Mech.* **25**, 657–682.

CRUM, G. F. & HANRATTY, T. J. 1965 Dissipation of a sheet of heated air in a turbulent flow. *Appl. Sci. Res.* A **15**, 177–195.

CSANADY, G. T. 1966 Dispersal of foreign matter by the currents and eddies of the Great Lakes. *Pub. No. 15 Great Lakes Res. Div. Univ. Michigan* (*Proc. 9th Conf. on Great Lakes Res.*), pp. 283–294.

CSANADY, G. T. 1967 Concentration fluctuation in turbulent diffusion. *J. Atmos. Sci.* **24**, 21–28.

CSANADY, G. T. 1980 *Turbulent Diffusion in the Environment*, pp. 222–248. D. Reidel.

CSANADY, G. T., HILST, G. R. & BOWNE, N. E. 1968 Turbulent diffusion from a cross-wind line source in shear flow at Fort Wayne, Indiana. *Atmos. Environ.* **2**, 273–292.

DURBIN, P. A. 1980 A stochastic model of two-particle dispersion and concentration fluctuations in homogeneous turbulence. *J. Fluid Mech.* **100**, 279–302.

FACKRELL, J. E. & ROBINS, A. G. 1982 Concentration fluctuations and fluxes in plumes from point sources in a turbulent boundary layer. *J. Fluid Mech.* **117**, 1–26.

GAD-EL-HAK, M. & MORTON, J. B. 1979 Experiments on the diffusion of smoke in isotropic turbulent flow. *AIAA J.* **17**, 558–562.

HINZE, J. O. 1975 *Turbulence.* McGraw-Hill.

KALINSKE, A. A. & PIEN, C. L. 1944 Eddy diffusion. *Ind. Engng Chem.* (Intl Edn), **36**, 220–223.

KAMPE DE FERIET, J. 1938 Some recent researches on turbulence. In *Proc. 5th Intern. Cngr. Appl. Mech. Cambridge, Mass.*, pp. 352–355.

LAMB, R. G. 1981 A scheme for similating particle pair motions in turbulent fluid. *J. Comp. Phys.* **39**, 329–346.

LEE, J. & BRODKEY, R. S. 1963 Light probe for the measurement of turbulent concentration fluctuations. *Rev. Sci. Instrum.* **34**, 1086–1090.

LEE, J. L. & BRODKEY, R. S. 1964 Turbulent motion and mixing in a pipe. *AIChE. J.* **10**, 187–193.

LUNDGREN, R. S. 1981 Turbulent pair dispersion and scalar diffusion. *J. Fluid Mech.* **111**, 27–57.

MACCARTER, R. J., STUTZMAN, L. F. & KOCH, H. A. 1949 Temperature gradients and eddy diffusivities in turbulent fluid flow. *Ind. Engng Chem.* **41**, 1290–1295.

MICKELSEN, W. R. 1960 Measurements of the effect of molecular diffusivity in turbulent diffusion. *J. Fluid Mech.* **1**, 397–400.

MURTHY, C. R. & CSANADY, G. T. 1971 Experimental studies of relative diffusion in Lake Huron. *J. Phys. Oceanogr.* **1**, 17–24.

NAKAMURA, I., MIYATA, M. & SAKAI, Y. 1983 On a method of the concentration measurement by the use of light absorption law. *Bull. JSME* **26**, 1357–1365.

NAKAMURA, I., SAKAI, Y., MIYATA, M. & TSUNODA, H. 1986 Diffusion of matter from a continuous point source in uniform mean shear flows (1st report, Characteristics of the mean concentration field). *Bull. JSME* **29**, 1141–1148.

NYE, J. O. & BRODKEY, R. S. 1967*a* The scalar spectrum in the viscous-convective subrange. *J. Fluid Mech.* **29**, 151–163.

NYE, J. O. & BRODKEY, R. S. 1967*b* Light probe for measurements of turbulent concentration fluctuations. *Rev. Sci. Instrum.* **38**, 26–28.

RAMSDELL, J. W. & HINDS, W. T. 1971 Concentration fluctuations and peak to mean concentration ratios in plumes from a ground-level continuous point source. *Atmos. Environ.* **5**, 483–495.

SAKAI, Y. 1984 Experimental study on the turbulent diffusion of matter by light-absorption method. Ph.D. thesis, Nagoya University (in Japanese).

SAKAI, Y., NAKAMURA, I., MIYATA, M. & TSUNODA, H. 1986 Diffusion of matter from a continuous point source in uniform mean shear flows (2nd report, Characteristics of concentration fluctuation intensity). *Bull. JSME* **29**, 1149–1155.

SAWFORD, B. L. 1983 The effect of Gaussian particle-pair distribution fluctuations in the statistical theory of concentration fluctuations in homogeneous turbulence. *Q. J. R. Met. Soc.* **109**, 339–354.

SREENIVASAN, K. R., TAVOULARIS, S., HERRY, R. & CORRSIN, S. 1980 Temperature fluctuations and scales in grid-generated turbulence. *J. Fluid Mech.* **100**, 597–621.

STAPOUNTZIS, H., SAWFORD, B. L., HUNT, J. C. R. & BRITTER, R. E. 1986 Structure of the temperature field downwind of a line source in grid turbulence. *J. Fluid Mech.* **165**, 401–424.

TAYLOR, G. I. 1921 Diffusion by continuous movements. *Proc. Lond. Math. Soc.* **20**, 196–212.

TENNEKES, H. & LUMLEY, J. L. 1979 *A First Course in Turbulence.* MIT Press.

TOWLE, W. L. & SHERWOOD, T. K. 1939 Eddy diffusion, mass transfer in the central portion of a turbulent air stream. *Ind. Engng Chem.* **31**, 457–462.

TOWLE, W. L., SHERWOOD, T. K. & SEDER, L. A. 1939 Effect of a screen grid on the turbulence of an air stream. *Ind. Engng Chem.* **31**, 462–463.

TOWNSEND, A. A. 1954 The diffusion behind a line source in homogeneous turbulence. *Proc. R. Soc.* Lond. A **224**, 487–512.

UBEROI, M. S. & CORRSIN, S. 1953 Diffusion of heat from a line source in isotropic turbulence. *NACA Rep. No. 1142.*

WARHAFT, Z. 1984 The interference of thermal fields from line sources in grid turbulence. *J. Fluid Mech.* **144**, 363–387.

YAMAMOTO, K. & SATO, Y. 1979 Measurements of Lagrangian behaviors of turbulent fluid. *Study of Fundamental Engineering for Materials in Yokohama National University*, no. 14, pp. 25–36 (in Japanese).

YEH, T. T. & VAN ATTA, C. W. 1973 Special transfer of scalar and velocity fields in heated-grid turbulence. *J. Fluid Mech.* **58**, 233–261.